Int. J. Electrochem. Sci., 14 **(2019)** 9355 – 9368, doi: 10.20964/2019.09.52

International Journal of
ELECTROCHEMICAL
SCIENCE
www.electrochemsci.org

Electrochemical Preparation of Iron-Supported Carbon-Cloth Electrode and Its Application in the In-Situ Production of Hydrogen Peroxide

Ikenna Chibuzor Emeji[1], *Onoyivwe Monday Ama*[2, 3,] Peter *Ogbemudia Osifo*[1], *Suprakas Sinha Ray*[2, 3], *Orlando García-Rodríguez*[4], *Olivier Lefebvre*[4]

[1] Department of Chemical Engineering, Vaal University of Technology, Private Mail Bag X021, Vanderbijlpark 1900, South Africa.
[2] Department of Applied Chemistry, University of Johannesburg, Doornfontein 2028, South Africa.
[3] DST/CSIR National Centre for Nano-structured Materials, Council for Scientific and Industrial Research, Pretoria 0001, South Africa.
[4] Centre for Water Research, Department of Civil and Environmental Engineering, National University of Singapore, No. 1 Engineering Dr. 2, Singapore, 117576.
*E-mail: emejiiyk@gmail.com, onoyivwe4real@gmail.com

Received: 6 March 2019 / *Accepted:* 12 July 2019 / *Published:* 5 August 2019

This study describes how carbon-cloth (CC) electrode was demonstrated to have good electrical conductivity using linear sweep voltammetry (LSV). Its electrocatalytic activity was evaluated toward the generation of hydrogen peroxide (H_2O_2) via oxygen reduction reaction by two electrons. Electrochemical deposition of iron on an electrode surface was vital in the synthesis of iron modified carbon-cloth electrode, in that the process was used to eliminate iron salts in solution as precursors for the homogeneous Fenton process because of its large solid sludge formation. Iron electrodeposition potential was found to be; -1.3 V ≦ E ≦ 1.00 V and -1.8 V to 1 V. Chronoamperometry technique was successfully used to deposit 0.1M of iron on the CC electrode. The following materials synthesised, iron supported carbon-cloth electrodes were characterised. Using a scanning electron microscope (SEM) and energy dispersive X-Ray spectroscopy (EDX) analysis, the morphology, elemental distribution, and composition of the modified CC electrode were observed. The availability of oxygen-containing functional groups on the modified electrode was confirmed by X-ray photoelectron spectroscopy (XPS) analysis. These functional groups on CC electrode act as oxygen reduction reaction (ORR) active sites for in-situ H_2O_2 promotion, electro-generation, and activation. Hence, the magnitudes of nitrogen-to-carbon (N/C) and oxygen-to-carbon (O/C) ratios were calculated to be 0.02% and 0.29% respectively, indicating high oxygen content as compared to nitrogen. Therefore, the techniques and application of using low-cost carbon-cloth materials, to support iron particles, for in-situ hydrogen peroxide generation suggest innovation.

Keywords: Hydrogen peroxide (H_2O_2), Carbon-cloth electrode, Oxygen reduction reaction (ORR), Electrodeposition,

1. INTRODUCTION

Hydrogen peroxide (H_2O_2) is an ecologically benign oxidant and one of those chemicals used in advanced oxidation processes (AOPs) for water and sewage decontamination [1]. The use of H_2O_2 has offered an efficient alternative for the obliteration of organic and inorganic contaminants in aqueous media. Although hydrogen peroxide is profitably produced on a commercial scale by anthraquinone process, the process is rigorous and generates a significant volume of liquid wastes. In addition, the product must be handled and transported to the work site, posing a safety risk. Therefore, hydrogen peroxide produced using this technique, encompasses a significant environmental influence, which is in contrast to green chemistry principles [2]. As a result, a replacement for H_2O_2 production follows the pathway of two-electron oxygen reduction reaction (ORR) in acidic, basic or neutral media as shown in equation 1 and 2 [3] [4]. ORR can also occur by a direct process called 4e− process as depicted in equation 3 and 4 [4]. Hence, the on-site generation of sustainable hydrogen peroxide requires the operations of air (oxygen), water and electricity, which could be provided from renewable sources. Generally, the use of Fenton's reagent in recent times, as an oxidative degradation tool is very attractive because iron is a non-toxic element and easily available. In addition, H_2O_2 breaks down to environmentally harmless products of hydrogen and water (equation 5) [5] [6]. However, homogeneous Fenton technology has its limitations, in the massive ferric-hydroxide sludge formation [6] at pH greater than 4.0 and the complication arising from the transportation, handling, and storage of H_2O_2 [7]. To overcome these limitations to some extent, heterogeneous catalysts are used. Hence, in a heterogeneous Fenton process, iron is fixed or immobilised within the catalyst structure and reaction occurs on the surface interfaces of the solid catalyst-electrode and the conducting solution. Therefore, an apparent adsorption and diffusion process of H_2O_2 on the surface of electrode enhances catalytic reaction [8]. Punzi and co-workers [9] also reported that the slower step of the heterogeneous catalytic system, as compared to their homogeneous counterpart, could be as a result of an electrodeposited small fraction of iron on the surface of the catalyst.

O_2 (g) + $2H^+$ + $2e^-$	⟶	H_2O_2 (acidic)	(1)
O_2 (g) + $2H_2O$ + $2e^-$	⟶	H_2O_2 + $2OH^*$ (basic)	(2)
O_2 (g) + $4H^+$ + $4e^-$	⟶	$2H_2O$ (acidic)	(3)
O_2 (g) + $4H^+$ + $4e^-$	⟶	$4OH^*$ (basic)	(4)
H_2O_2	⟶	O_2 + H_2O	(5)
Fe^{2+} + H_2O_2	⟶	Fe^{3+} + OH^- + OH^*	(6)
Organics + OH^*	⟶	Oxidation intermediates + CO_2 + H_2O	(7)

Several authors such as Peralta-Hernández [10], Martínez-Huitle and Brillas [11] have demonstrated that in-situ electro-generated H_2O_2 can be used successfully to separate micro-pollutants from water effluents contaminated with different organic compounds in an aqueous or a non-aqueous medium. The principle of decontamination, however, is initiated through Fenton reaction (equation 6) [6] [12], as in-situ electrochemical generated peroxide reacts with ferrous ions (Fe^{2+}) to produce hydroxyl radicals (OH*****), which can efficiently mineralise recalcitrant organic micro-pollutants

contained in wastewater as shown by equation 7 [13]. This technique, frequently called electro-Fenton (EF) is an advanced oxidation process (AOP) because of the creation of active hydroxyl radicals (OH*), a very strong reactive oxidant with high oxidation potentials of 2.8 V. Hence, the use of carbonaceous materials as electrode materials are found to catalyse oxygen reduction reaction (ORR) selectively by two electrons using appropriate cathodic potential, in an electrolytic solution enriched with oxygen forming hydrogen peroxide. Apart from electrode materials, another inhibiting consideration in the capability of hydrogen peroxide production through ORR is the high insolubility of oxygen in water at room temperature. Hence, the use of gas diffusion electrode (GDE) overcomes the high insolubility of oxygen, which causes mass transfer limitations at the cathode surface. It is imperative that carbon-based materials such as glassy carbon modified with palladium nanoparticles [14], activated carbon [15], carbon nanotubes (CNTs) [16] and nitrogen-doped mesoporous carbon [17], have shown great promise as alternative catalysts for the electrochemical production of hydrogen peroxide. Despite progress in the synthesis of carbon-based electrodes, there is stil lroom for improvement in modifying and developing carbon-based substances for in-situ hydrogen peroxide production. In this study, we analysed the electrocatalytic activity and selectivity of carbon-cloth and iron supported carbon-cloth electrode toward the production of in-situ H_2O_2 using surface oxidation.

2. MATERIALS AND METHODS

2.1 Materials and Apparatus

Potassium sulphate (K_2SO_4), sulphuric acid (H_2SO_4), iron (II) sulphate heptahydrate ($FeSO_4 \cdot 7H_2O$), and titanium (IV) oxy-sulphate ($TiOSO_4$, 15 wt. % in dilute sulphuric acid and purity of 99.99% trace metals basis), were all purchased from Sigma-Aldrich, South Africa. All reagents used were prepared with high purity water (Millipore Milli-Q, 18 M cm). Carbon-cloth electrode was purchased from Fuel Cell Earth, Massachusetts, United States. AGA, South Africa supplied oxygen and nitrogen gasses. The characterisations of the CC electrode were carried out using the following techniques: scanning electron microscopy (SEM), energy-dispersive x-ray spectroscopy (EDX) and x-ray photoelectron spectroscopy (XPS) microanalysis. Hydrogen peroxide was generated in-situ using electrolysis experiment which was carried out in a 250 ml capacity cell containing 50 mM (millimole) K_2SO_4 aqueous electrolyte at a PH of 3, bare or modified CC electrode (12.5 cm^2) as the working cathode and platinum wire (Pt.) as the anode. Hailea air-pump was used to oxygenate the electrolyte and HM8040-3 triple-power supplier supply's required current to the system. UV–vis spectrophotometer (Perkin Elmer model Lambda 35) was used to measure the absorbance of the intense yellow coloration of stable pertitanic acid complexes formed by the reaction between hydrogen peroxide and titanium (IV) oxy-sulphate. An Autolab potentiostat/galvanostatic was employed during electrode conductivity text, iron reduction potential experiment and electrodeposition.

2.2 Linear Sweep Voltammetry (LSV) Measurement for ORR

A conductivity experiment for the carbonaceous electrode was done in a three-electrode electrochemical cell consisting of CC electrode (12.5 cm^2) as the working electrode (WE), platinum wire and Ag/AgCl as the counter electrode (CE) and a reference electrode (RE), respectively. Cell-connecting cables with crocodile clips were used to clip the heads of the electrodes (WE, CE and RE) and connect the other head to a potentiostat. LSV measurement was carried out at room temperature in 50 mM K_2SO_4 electrolytic solution at a pH of 3.While the first LSV scan was carried out in electrolyte enriched with O_2/air for 35 minutes; the second linear sweep was carried in deoxygenated electrolyte achieved by pumping N_2 gas into the solution for 35 minutes. The LSV scan tested the electrode for 300 seconds (5minutes), using an electrochemical potential range of -1.5 V ≦ E≦ 1.00 V at a scan rate of 0.05 V/s.

2.3 Evaluation of Iron Reduction Potential through Cyclic Voltammetry (CV) Measurement

The iron reduction potential experiment was also performed using a three-electrode electrochemical cell consisting of CC electrode (12.5 cm^2) as the working electrode (WE), platinum wire and Ag/AgCl as the counter electrode (CE) and a reference electrode (RE), respectively. Through the Teflon-cap of the cell cover, two tiny stainless-steel wires were used to hold the CC-working electrode and the platinum counter electrode firmly. Connecting cell cables with three crocodile clip heads were used to hold the heads of WE, CE and RE with the other end connected to the potentiostat. CV measurements were performed at room temperature in 50mM K_2SO_4 solution at a pH of 3 containing 0.1M 100ml $FeSO_4.7H_2O$. The electrolyte was only enriched with N_2 gas for 35 min prior to the experiment. Here, the electrode was tested for 180 seconds, using the following potential sweep window of -0.8 V ≦ E≦ 1.00 V; -1.3 V ≦ E ≦ 1.00 V and -1.8 V to 1 V; and a scan rate of 0.05 V/S. When adding the electrolyte into the cell, it was done by means of a thistle funnel, in such a way that the WE was completely immersed in the solution.

2.4 Preparation of Iron-Supported CC Electrode by Electrodeposition

Reagent grade iron (II) sulphate heptahydrate ($FeSO_4.7H_2O$) was used to prepare 0.1 M 100mL iron (II) sulphate solution using 50 mM, N_2-gas enriched K_2SO_4electrolyte at a pH of 3.0. The electrochemical setup for electrodeposition was a standard three-electrode cell with 12.5 cm^2carbon cloth as the working electrode, platinum as the counter electrode and silver-silver chloride as the reference electrode. Two stainless steel wires passing through two separate smallest holes on the cell cover were used to hold WE and the CE externally. Through another hole on the cell cover, closer to the WE, Ag/AgCl reference electrode (RE) was inserted and by means of a thistle funnel, pour about 10 ml of the prepared iron (II) solutions into the cell. The electrodeposition of iron on the surface of the electrode was performed during chronoamperometry using Autolab potentiostat/galvanostat PGSTAT 302F. Iron particles were deposited by cyclic sweeping from -1.8 to 1 V and back at 0.05V/s for 90 cycles in 0.1M $FeSO_4.7H_2O$ containing 50 mM (millimole) of K_2SO_4 solution. The modified electrodes

were rinsed with high purity water and air dried, after which they were characterised using SEM analysis, EDX analysis and XPS analysis.

2.5 Electrochemical Generation of in-situ H_2O_2

Electrolysis experiment enables the determination of the maximum concentration of H_2O_2 electro-generation within the system. It also enables current to be optimised at maximum peroxide concentration. The H_2O_2 electro-generation experiment was performed in an undivided glass cell of 250 ml capacity using an air pump and HM8040-3 triple-power supply. The modified iron-supported CC electrode (2.5 x 5 cm) was selected as the cathode and a platinum wire was employed as the anode. Using stainless-steel wire, the electrodes were held firmly in such a manner that they were 2 cm from the bottom of the glass cell and 2 cm from one another. Prior to the electrolysis experiment, compressed air (oxygen) was used to saturate 0.05M K_2SO_4 aqueous electrolyte using the air pump for about 35 minutes. By transferring the aeration-tube near the cathodic surface, an essential amount of oxygen was supplied for the electrochemical reactions; electrolyte oxygenation was maintained with a constant magnetic stirrer of 300 rpm. Oxygen was reduced by applying a constant electric current (I = 0.05A, 0.025A and 0.0125A) on the surface of the working electrode for 60 minutes. Sampling was done every 10 minutes by means of an Eppendorf micro-pipette. The concentration of H_2O_2 electro-generated during the process (C) was quantified by photoelectric measurement, measuring the absorbance of the colour complex intensity of hydrogen peroxide solution treated with titanium oxy-sulphate at a wavelength of 405 nm using a UV-Vis spectrophotometer [18] [19].

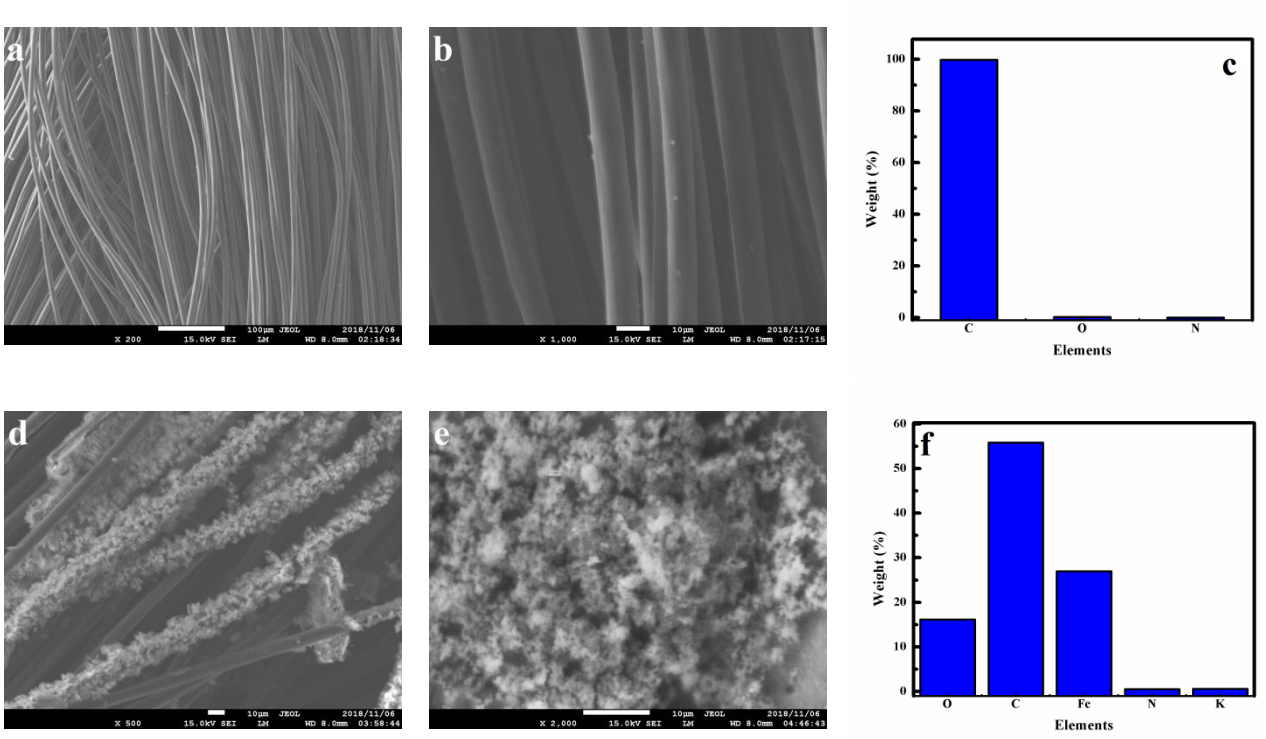

Figure 1. (a) SEM of bare-CC electrode, (b) SEM of bare-CC electrode showing lumps as impurities, (c) EDX of bare-CC electrode, (d) SEM of iron-supported CC electrode, not completely covered, (e) SEM of iron-supported CC electrode, uniformly covered, and (f) EDX of iron-supported CC electrode

The current efficiency (CE) for H_2O_2 generation was calculated with the formula [20] [21].

$$\boldsymbol{CE = \frac{2FCV}{\int_0^t Idt} \times 100\%} \quad \textbf{(6)}$$

Where F is the Faraday constant, equal to 96500 C/mol, C is the concentration of H_2O_2 in mol/L, V is the solution volume (L), I is the applied current (A), and t is the production time (s). The electric energy consumption (EEC) (kWh/m^3) was calculated using the formula [21].

$$\boldsymbol{EEC = \frac{U\,I\,t}{V}} \quad \textbf{(7)}$$

Where U represents the applied voltage (V), I the current (A), t the treatment time (h) and V is the solution volume (m^3)

3. RESULT AND DISCUSSION

3.1 Characterisation Result

After electrodeposition, the electrode surface substantially changes. Using SEM analysis, the morphological characteristics of the electrode surface was inspected as depicted in Figure 1 (a, b, d and e). Figure 1a shows that the untreated bare-CC electrode had a porous structure with overlapping carbon fibres. The carbon fibre has a very smooth surface with irregular small lumps attached to it, as shown in Figure 1b. These attachments may have been some contaminant and could be removed through pre-treatment with acid and alkali. Figure 1d and 1e show that after electrodeposition, iron particles were deposited and well dispersed on the surface of CC electrode, making their surface rough. This means that the CC electrode has high porosity and consequently, good adsorption capacity. As shown in Figure 1d, the iron deposit was not completely uniform as observed in some places of the bare carbon-cloth electrode. However, in Figure 1e, the coverage was uniform over the carbon cloth lattice. This structure was expected to help enhance electrochemical activity and the mass-transfer process of ORR by $2e^-$, leading to the generation of in-situ H_2O_2. The (EDX result as shown in Figure 1 (c & f) and Table 1, confirms the elemental composition of the electrode surface.

Table 1. EDX result of bare and iron-supported CC electrode

Samples	Weight %				
	Carbon	Oxygen	Nitrogen	Potassium	Iron
Fe / CC Electrode	55.79	16.14	0.53	0.58	26.96
Bare Electrode		99.74	0.22	0.04	

Based on the result, the presence of C, O and N was confirmed on the bare CC electrode. In addition, the presence of different weight % of Fe was confirmed in the structure of the modified

electrode. Based on the EDX results, the magnitudes of nitrogen-to-carbon (N/C) and oxygen-to-carbon (O/C) ratios were calculated to be 0.009% and 0.29% after electrodeposition on the surface of the electrode. The calculated result shows that the resultant modified electrode has high oxygen content as compared to nitrogen, which confirmed the adsorption of iron onto the CC electrode surface after electrodeposition. Another surface analysis which determines the atomic composition of the electrode was X-ray photoelectron spectroscopy (XPS) analysis as shown in Figure 2.

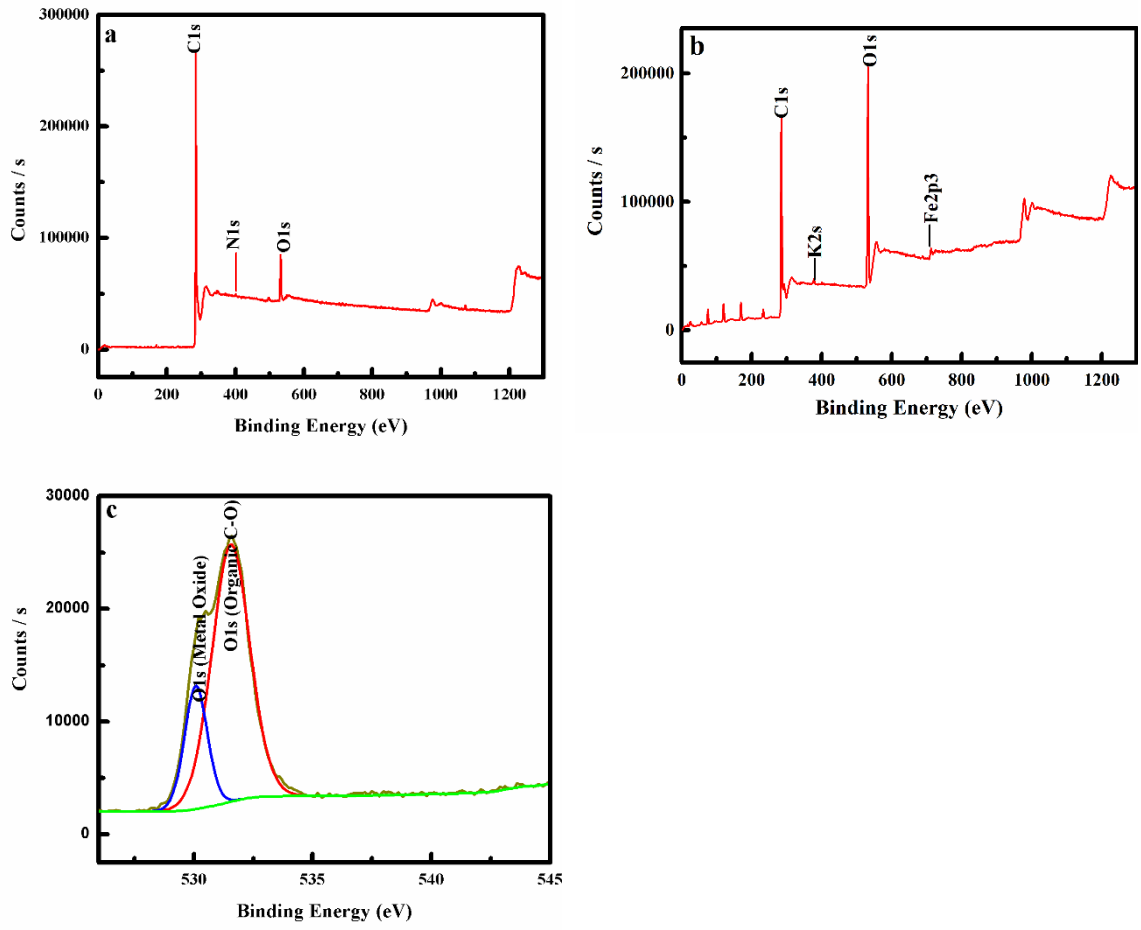

Figure 2. XPS analysis of (a) Bare-CC electrode, (b) Iron-supported CC electrode and (c) High-resolution spectra of iron-supported CC electrode

It can be seen from Figure 2a, that the bare-CC electrode has three detectable peaks: one at 284.3 eV, which corresponds to carbon C1s, another at 532.1 eV corresponding to oxygen O1s and the last at 400.7 eV corresponding to nitrogen N1s. The modified electrode presented an extra peak at 711.3 eV, corresponding to the iron Fe2p3 particles and 377.8 eV corresponding to the potassium K2s. For the coated CC electrode, a high-resolution XPS spectrum of O1s shows the presence of an additional functional group of O1s (metal oxide) (530.1 eV) and O1s (organic C-O) (531.6 eV). The existence of these oxygen-containing functional groups in the carbon-cloth electrode provided more active sites, which enhances the catalytic activity for the promotion and generation of H_2O_2. This result agrees with

Zhong [22], which suggested that the surface reduction/modification of carbon support produces more active and anchor sites for the enhancement of ORR catalytic activities. Also, agreeing with this assertion is Ananth and co-workers [23], who reported that the protection of crystalline structures and the presence of additional surface oxygen-containing functional groups improve ORR activity.

3.2 Electrochemical generation of in-situ H_2O_2in the Electrochemical Cell

LSV experiments were carried out to examine the ability of the CC electrode to create H_2O_2through the cathodic reduction of diffused O_2 in a 50mM solution of K_2SO_4 electrolyte altered to a pH of 3 with H_2SO_4. LSV curves for CC electrode are presented in Figure 3.

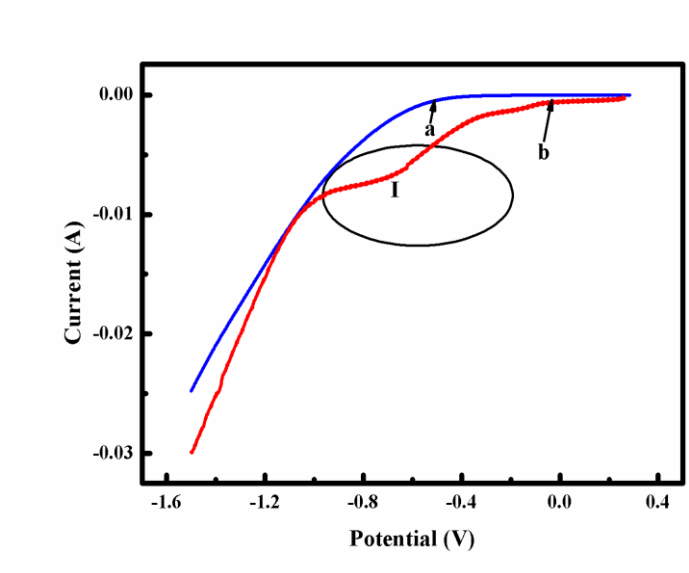

Figure 3. LSV response of CC electrode immersed in (a) O_2-saturated (b) N_2-saturated, 50 mM K_2SO_4 solution, Scan rate = 0.05V/s

The CC electrode discloses good ORR activity in the oxygen-enriched electrolyte (curve b), and relatively poor activity in nitrogen enriched electrolyte (curve a). The oxygen reduction potentials for the CC electrode were detected at -0.65V, within the circled region. Although oxygen reduction reaction is recognised to progress through two and four electron pathways, as presented in equation 1, 2, 3 and 4, the use of carbonaceous material, selectively enables the two-electron pathway thus favouring the production of in-situ H_2O_2 [24]. However, the route of oxygen reduction is firmly based on the type of electrode material. The surface chemistry and the majority of the electrode's crystalline structure are responsible for the perceived excellent oxygen reduction capabilities. The LSV results have, therefore, demonstrated that the CC electrode conducts electricity (conductive) and had a stronger ORR catalytic activity in oxygen-enriched electrolyte for H_2O_2 production.

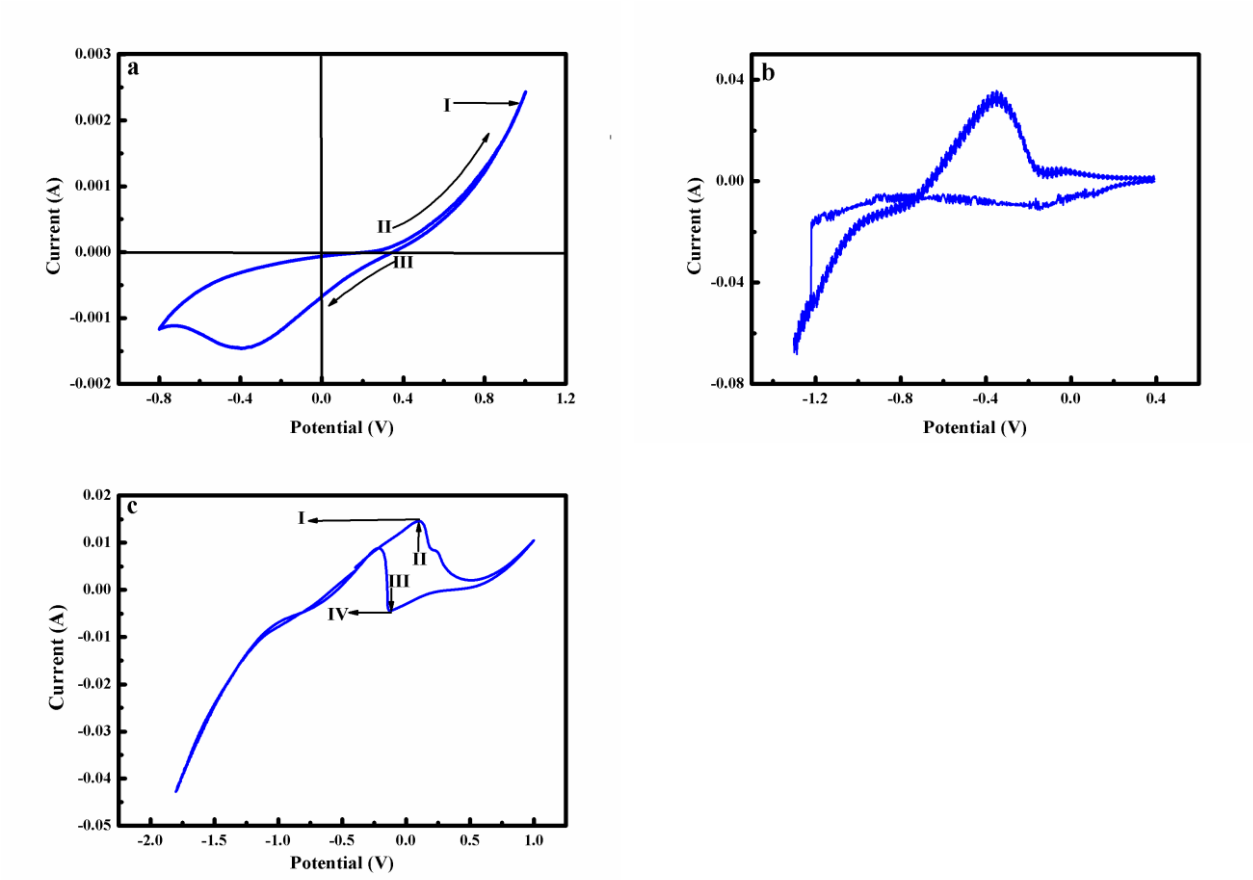

Figure 4. CV measurement of CC electrode in N_2-saturated 50 mM K_2SO_4 solution, at a pH of 3 containing 0.1M 100ml $FeSO_4.7H_2O$. Scan rate = 0.05V/s

On another development, Figure 4 (a-c) depicts the CV measurement which was carried out to evaluate iron reduction potentials for successful electrodeposition. Figure 4a reveals that during the potential sweep of -0.8V < E < 1 (vs Ag/AgCl), there was no observable peak for the oxidation and reduction reaction in the electrochemical cell. This is an indication that the electrode needs a wider potential window within which to operate. The rapid increase in current as shown by arrow-I was attributed to the electrochemical decomposition of the electrolyte (K_2SO_4). As iron species are initially present in the solution competing with potassium ions for active sites, a further negative potential sweep (-1.3 V vs Ag/AgCl) results in a cathodic reduction process on the electrode surface. This results in the desire of the system to set-up an equilibrium directed by the applied voltage. Hence, in Figure 4b, it was observed that the shape of the forward reduction peak is not identical to the shape of the oxidation peak for the reverse sweep. This indicates that iron reduction and oxidation rates are not equal, indicating successful electrodeposition at this potential. Improved electrodeposition was observed in Figure 4c at a potential sweep of -1.8 V to 1 V vs Ag/AgCl). The voltammograms resulting from this potential scan show similarity in shape between cathodic and anodic waves. The cathodic peak current and voltage were located at IV = - 4 mA and III = - 124 mV while the anodic peak current and voltage correspond to I = 15 mA and II = 102 mV. However, peak-to-peak potential difference greater than 200 mV ($\mathbf{\Delta E_p}$ > 200mV) indicates irreversibility [25]. The redox peak potential difference ($\mathbf{\Delta E_p} = E_p^c - E_p^a$) was 226 mV

indicating that the process is not reversible. Hence at the applied potentials of -1.8V < E < 1 (vs Ag/AgCl) and 1 V to -1.5 V (vs Ag/AgCl), the cyclic voltammetry (CV) measurement obtained with CC electrode indicates better morphological structure, as corroborated by the characterisation result. Thus, irreversibility of the process may probably be responsible for successful iron electrodeposition on the surface of the electrode.

3.3 Effect of current density on in-situ electro-generated H_2O_2

The effect of current density on H_2O_2 production, based on the study conducted using a UV-vis spectrophotometer is shown in Figure 5.

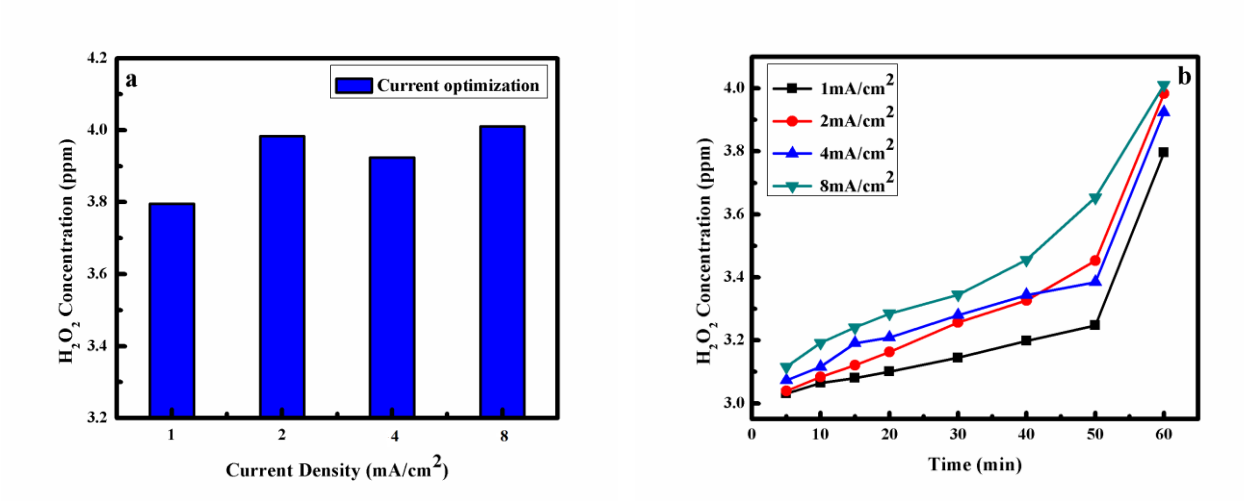

Figure 5. H_2O_2 production during electrolysis using triple power supplier in an O_2-saturated 50 mM K_2SO_4 solution, at a pH of 3 (a) at different current densities (b) at different reaction time.

The yield of H_2O_2 with the bare-CC electrode in 60 min at different current densities of 1, 2, 4 and 8 mA/cm^2 was 3.796, 3.983, 3.924 and 4.011 mg/L, respectively. For current densities of 1, 2, 4, and 8 mA/cm^2, it was observed that generated H_2O_2 concentration is directly related to the current density furnished to the system. This result conforms with previously reported results [18]. In the case of 4 mA/cm^2 current density application, the H_2O_2 concentration obtained was 3.924 mg/L (Figure 5a), a value lower than what was obtained when a current density of 2 mA/cm^2 was applied for 60 minutes.

A tenable clarification for this phenomenon lies in the mass transfer coefficient of H_2O_2 formation in the system, as explained by Peralta-Hernández and Godínez [26]. However, increased current density accelerates electron transfer on the CC electrode, promoting the oxygen reduction reaction. As a result, the higher current density can produce more in-situ H_2O_2 as depicted in Figure 5b. Petrucci and co-workers [27] reported a decrease in the generation of in-situ H_2O_2 when the current density is increased by a few milliamps per square centimeter (mAcm^{-2}) in plain carbonaceous materials. Pérez [28] also reported that applying current density higher than the limiting current density, could lead to the advancement of some side reactions, which compete with the generation and accumulation of

H_2O_2, like $4e^-$ reduction of O_2 to H_2O (equation 3) and peroxide decomposition [29] leading to oxygen evolution (Equation 5). Some researchers such as Barros [30] and Kolyagin [31] etc. have previously applied higher current density in the electrochemical generation of hydrogen peroxide with an excellent outcome. However, those results show that more research is needed for the advancement of hydrogen peroxide production using carbonaceous materials. It was reported that at high current density, current efficiency decreases and at low current density, current efficiency increases [27]. This is in agreement with the results obtained in this study, with the modified CC electrode given higher current efficiency.

3.4 Evaluation of the catalytic activity of CC electrode

The catalytic activity in the oxygen reduction reaction of CC electrode was carried out during the production of in-situ H_2O_2. Bare-CC electrode accumulated 4.011 mg/L of H_2O_2 in the electrochemical cell, as shown in Figure 5. The accumulated H_2O_2 in the cell is low, as compared to 8 mg/L result obtained by García-Rodríguez [18]. Though the in-situ generation of H_2O_2 was achieved by the bare-CC electrode, instability and self-decomposition of the resulting H_2O_2 molecule (equation 5) may be responsible for the low value of result obtained. The limitation of oxygen reduction reaction (ORR) on carbonaceous material may be another reason for the low generation of hydrogen peroxide in the electrochemical cell or lack of availability of an active site on the electrode surface for a surface reaction as proposed by Bañuelos [32]. After the analysis of bare-CC electrode, iron-supported CC electrode prepared by electrodeposition was used to determine the response of iron-metal to the amount of H_2O_2 accumulated in the electrochemical cell. As shown in Figure 6b, the H_2O_2 concentration increases linearly in the system with electrolysis time up to 60 minutes. The enhanced value of 36.939 mg/L of H_2O_2 was accumulated in the electrochemical cell for 60 minutes. Therefore the modified CC-electrode generated an outstanding amount of in-situ H_2O_2 of 36.939 mg/L as compared to the 4.011 mg/L generated by the bare CC electrode.

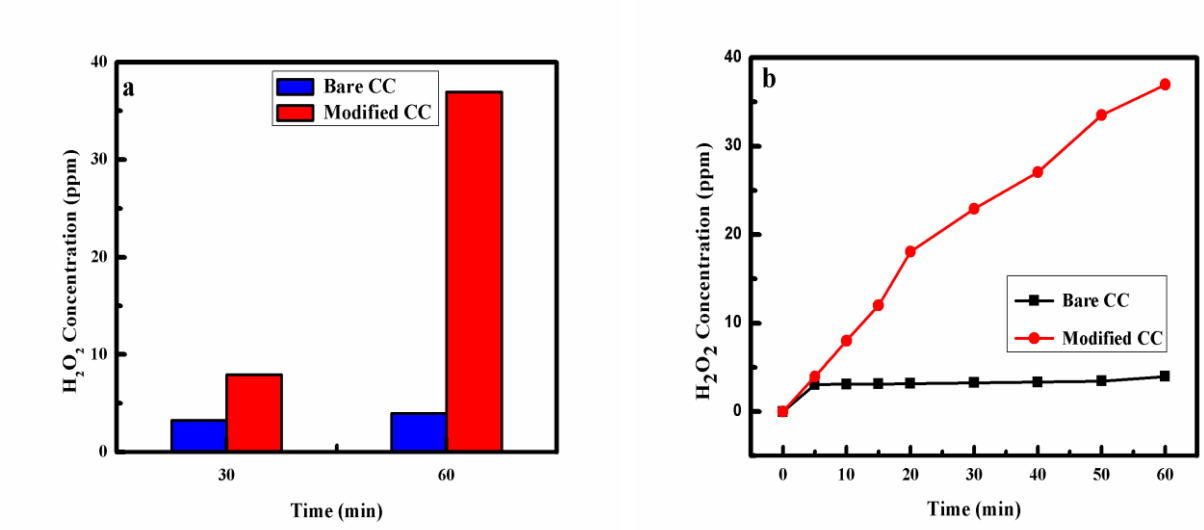

Figure 6. Performance of bare and iron-supported CC electrode for H_2O_2 accumulation by electrolysis using triple power supplier (a) at 30 and 60 minutes (b) against electrolysis time Vs Ag/AgCl

However, the generated amount of H_2O_2 in the electrochemical cell could be much higher than the spectrophotometrically measured amount. It has been reported that after iron electrodeposition on the surface of carbon-based electrode, zero-valent iron(ZVI)(Fe^0) was found to be electrodeposited on the material, which, through time, oxidises and generates Fenton reagent (equation 8), which, in turn reduces the accumulated amount of hydrogen peroxide as indicated by equation 6 [32]. Also, having a greater amount of iron present on the electrode surface (26.96 wt. %) as depicted by EDX analysis (Table 1) means that iron was interfering with the generated H_2O_2 to produce hydroxyl free radicals as indicated in equation 6, so the electrogenerated H_2O_2 was consumed as quickly as it was produced [32].

$$\mathbf{Fe^0 + O_2 + 2H^+ \longrightarrow Fe^{2+} + H_2O_2} \quad \mathbf{(8)}$$

Therefore, it is evident that iron-supported CC electrode exhibits higher catalytic activity and reaches a larger accumulation of H_2O_2 after electrodeposition than bare CC electrode. On a general note, oxygen-containing functional groups introduced on the surface of the electrode as corroborated by XPS analysis (Figure 3), could be responsible for higher catalytic activity for H_2O_2 enhancement. In comparison with other previously reported (Table 2), the modified CC electrode was found to be superior, and this implies that the iron-supported CC electrode used herein can be considered as an effective catalyst for in-situ hydrogen peroxide generation

Table 2. Performance of various supported CC electrode

Catalyst	Electrolyte	Con. of in-situ H_2O_2 generated (mg/L)	Reference
Carbon cloth modified with anthraquinone derivatives	KOH in Milli-Q water, saturated with O_2	Unreported data. Very low con. of H_2O_2 generated	[33].
carbon cloth modified with Pd/C and Ni/C	Formic acid with deionised water	Unreported data. Much smaller con. of H_2O_2 generated	[34].
carbon cloth modified with mesoporous carbon black	Na_2SO_4 enriched with oxygen	7.6	[35].
Carbon cloth modified with iron particles	K_2SO_4 enriched with oxygen.	36.7	[This work].

4. CONCLUSION

In this study, the CC electrode was found to be electrically conductive with a stronger ORR activity in the oxygen-enriched electrolyte for H_2O_2 production. Iron was used to modify the CC electrode by electrodeposition, after using CV measurement to determine iron deposition potential. Hence, the application of negative potential on electrode material promotes oxygen reduction reaction (ORR) via 2e- as verified by EDX analysis. After modification, characterisation analysis confirms a successful iron electrodeposited process on the surface of the carbon cloth electrode. More active and anchor sites were found to be present on the iron-supported CC electrode for ORR enhancement leading

to higher catalytic activity for the generation and accumulation of H_2O_2. On quantification, the concentrations of in-situ generated $H_2O_2$was found to be related to the current density furnished to the system. Although accumulated H_2O_2 concentration appears to be low, it could be that the generated amount of H_2O_2 was depleted by side reactions. Hence, modified iron supported CC electrode has a higher electrocatalytic activity of oxygen reduction reaction (ORR) via 2e- than bare CC electrode, thus providing an improvement in the initial production of H_2O_2.

ACKNOWLEDGMENTS
The authors express their sincere gratitude to Dr. Uyiosa Osagie Aigbe and Dr. Ephraim Igberase for their unflinching support; encouragement and assistance in making this study a reality.

References

1. V. Čolić, S. Yang, Z. Révay, I.E.L. Stephens and I. Chorkendorff, *Electrochim. Acta* 272 (2018) 192
2. A. Goti and F. Cardona, *Green Chem*. (2008) 191
3. L. Jiao-jiao, J. Wei, J. Cai and Y.X. Chen, *Chin. J. Chem. Phys*., 31(6) (2018) 779
4. Z. Zhou, A. Chen, A. Kong, X. Fan, X. Zhang and Y. Shan, *J. Electrochem. Soc*., 165 (2018) H658
5. D.I. Foustoukos, J.L. Houghton, W.E. Seyfried Jr, S.M. Sievert and G.D. Cody, *Geochim. Cosmochim. Acta,* 75(6)(2011) 1594
6. S.R. Pouran, A.A. Aziz and W.M.A.W. Daud, *J. Ind. Eng. Chem*., 21 (2015) 53
7. S. Qiu, D. He, J. Ma, T. Liu and T. D. Waite, *Electrochim. Acta*, 176 (2015) pp.51-58
8. C. Zhang, M. Zhou, G. Ren, X. Yu, L. Ma, J. Yang and F. Yu, *Water Res*., 70 (2015) 414
9. M. Punzi, B. Mattiassonand M. Jonstrup, *Photochem. Photobiol*., A, 248 (2012) 30
10. J.M. Peralta-Hernández, Y. Meas-Vong, F.J. Rodríguez, T.W Chapman, M.I. Maldonado and L.A. Godínez, *Dyes Pigm.,* 76 (2008)(3) 656
11. C.A. Martínez-Huitle and E. Brillas, *Appl. Catal*., B, 87 (2009) 105
12. Z. Heidari, M. Motevasel,and N.A. Jaafarzadeh, *Iranian Journal of Oil & Gas Science and Technology,* 4 (2015) 76
13. D.D.D. Aljuboury and P. Palanlandy, *Global NEST Journal*, 19 (2017) 641-649
14. S.A. Kitte, B.D. Assresahegnand T.R. Soreta, *J. Serb. Chem. Soc*., 78 (2013) 78
15. W. Zhou, L. Rajic, L. Chen, K. Kou, Y. Ding, X. Meng, Y. Wang, B. Mulaw, J. Gao, Y. Qin and A.N. Alshawabkeh, *Electrochim. Acta* 296 (2019) 317
16. Z. Lu, G. Chen, S. Siahrostami, Z. Chen, K. Liu, J. Xie, L. Liao, T. Wu, D, Lin, Y. Liu and T.F. Jaramillo, *Nat Catal*., 1 (2018) 156
17. Y. Sun, S. Li, Z.P. Jovanov, D. Bernsmeier, H. Wang, B. Paul, X. Wang, S. Kühl and P. Strasser, *ChemSusChem,* 11 (2018) 3388
18. O. García-Rodríguez, J.A. Bañuelos, A. Rico-Zavala, L.A. Godínez and F.J. Rodríguez-Valadez, *Int. J. Chem. React. Eng*., 14 (2016) 843
19. G. M. Eisenberg, *Ind. Eng. Chem., Anal. Ed*. 15, (1943) 327-328
20. Z. Qiang, J.H. Chang and C.P. Huang, *Water Research*, 36 (2002) 85
21. F. Yu, M. Zhou and X. Yu, *Electrochim. Acta,* 163 (2015) 182
22. H. Zhong, C. Campos-Roldán, Y. Zhao, S. Zhang, Y. Feng and N. Alonso-Vante, *Catalysts*, 8 (2018) 559
23. M.V. Ananth, V.V. Giridharand K. Renuga, *Int. J. Hydrogen Energy*, 34 (2009) 658
24. R. Reid, UWSPACE (2017)
25. H.C. Brookes and D. Inman, *ECS Proceedings Volumes* (1986) 128
26. J.M. Peralta-Hernández and L.A. Godínez, *J. Mex. Chem. Soc*., 58 (2014) 348

27. E. Petrucci, A. DaPozzo and L. DiPalma, *Chem. Eng. J.,* 283 (2016) 750
28. J.F. Pérez, C. Sáez, J. Llanos, P. Cañizares, C. López and M.A. Rodrigo, *Ind. Eng. Chem. Res*., 56 (2017) 12588
29. A. Vázquez, L. Alvarado, I. Lázaro, R. Cruz, J.L. Nava and I. Rodríguez-Torres, *Int. J. Photoenerg*, 2018
30. W.R. Barros, T. Ereno, A.C. Tavares and M.R. Lanza, *ChemElectroChem*, 2 (2015), 714
31. G.A. Kolyagin and V.L. Kornienko, *Russ. J. Appl. Chem*., 84 (2011) 68
32. J.A. Banuelos, O. García-Rodríguez, F.J. Rodríguez-Valadez, J. Manríquez, E. Bustos, A. Rodríguez and L.A. Godínez, *J. Appl. Electrochem*., 45 (2015) 523
33. E. Lobyntseva, T. Kallio, N. Alexeyeva, K. Tammeveski and K. Kontturi, *Electrochim. Acta*., 52(2007)25
34. Z. Fan, Y.H. Kwon, X. Yang, W. Xu, and Z. Wu, *Energy Procedia*, 105 (2017)
35. I. Papagiannis, E. Doukas, A. Kalarakis, G. Avgouropoulos and P. Lianos, *Catalysts*, 9 (2019) 3